

advances.sciencemag.org/cgi/content/full/6/9/eaay2915/DC1

Supplementary Materials for

The role of Northeast Pacific meltwater events in deglacial climate change

Summer K. Praetorius*, Alan Condron, Alan C. Mix, Maureen H. Walczak, Jennifer L. McKay, Jianghui Du

*Corresponding author. Email: spraetorius@usgs.gov

Published 26 February 2020, *Sci. Adv.* **6**, eaay2915 (2020)
DOI: 10.1126/sciadv.aay2915

The PDF file includes:

- Fig. S1. Modeled SSS, sea-ice, and SST anomalies in the deglacial simulation with an open Bering Strait for model years 5, 10, and 15.
- Fig. S2. Planktic $\delta^{18}\text{O}$ records from the Northeast Pacific.
- Fig. S3. Compilation of Northeastern Pacific B-P radiocarbon age differences from the LGM through the early Holocene.
- Fig. S4. Compilation of Northeastern Pacific subsurface ventilation records from the LGM through the early Holocene [with $\Delta^{14}\text{C}$ (%)] instead of B-P age differences.
- Fig. S5. SST measurements for ODP cores 1019C and 1019A on the original mean core depth splice (red, 1019C; green, 1019A) show misalignment near the Holocene transition by ~30 cm and the BA and YD transitions by ~5 cm.
- Fig. S6. Compilation of Northeast Pacific UK'37 SST reconstructions on age models with constant marine reservoir correction, in comparison with annual layer counted chronologies of the Greenland ice cores (46, 53) and the absolute U-Th chronologies of the western U.S speleothem records (69–71).
- Table S1. A revised mean composite depth for the upper 8 m of ODP core 1019A based on a revised correlation of GRA and MS data to the other cores within the splice for the upper 7 m.
- Table S2. Proxy data used for the global SST anomaly maps in Fig. 5 [(38, 45, 83–165) listed in alphabetic order].

Other Supplementary Material for this manuscript includes the following:

(available at advances.sciencemag.org/cgi/content/full/6/9/eaay2915/DC1)

- Data file S1 (Microsoft Excel format). Northeast Pacific SST data.
- Data file S2 (Microsoft Excel format). Northeast Pacific oxygen isotope data.
- Data file S3 (Microsoft Excel format). Northeast Pacific radiocarbon data.
- Data file S4 (Microsoft Excel format). Metadata for global SST compilation.

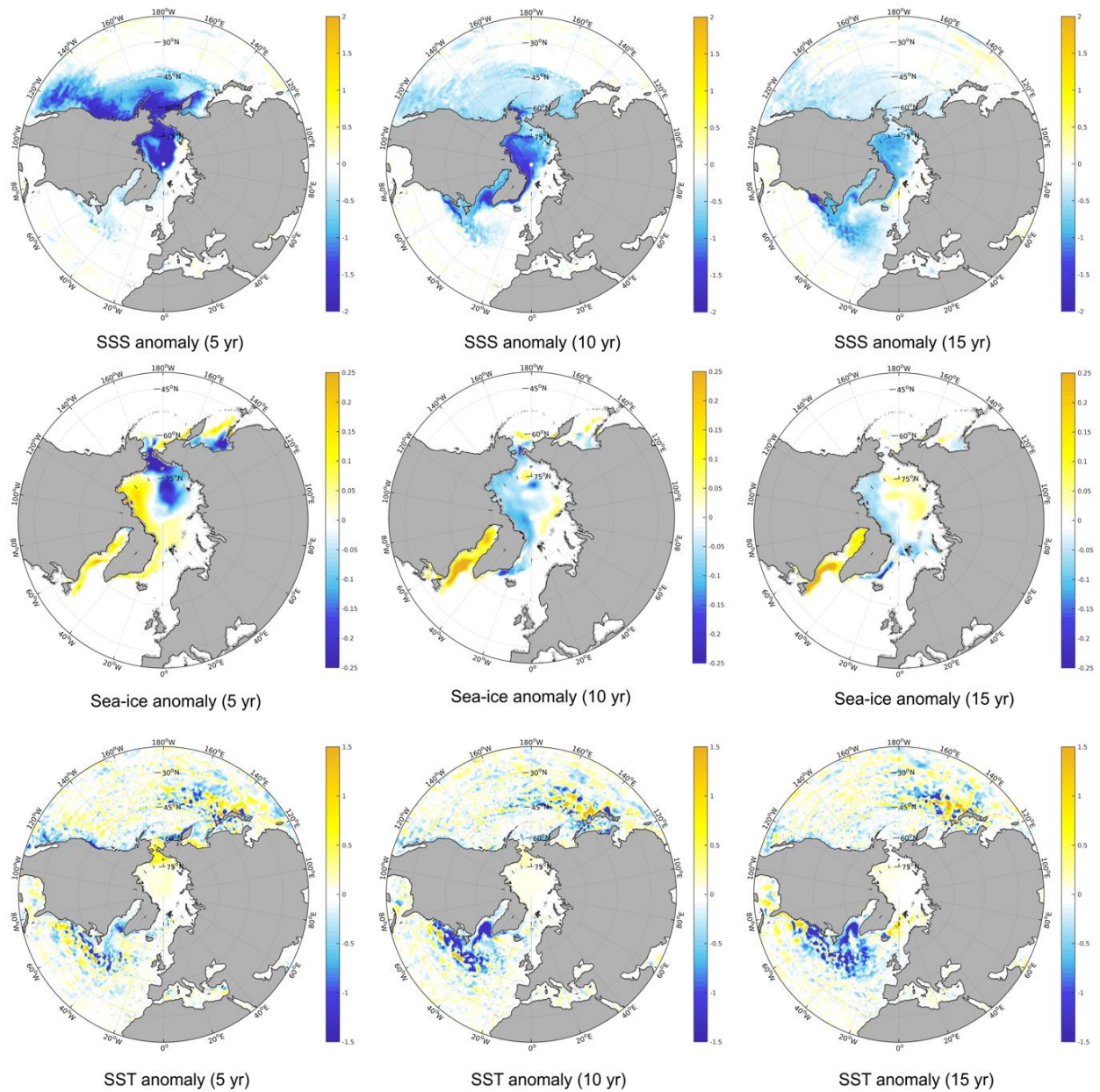


Fig. S1. Modeled SSS, sea-ice, and SST anomalies in the deglacial simulation with an open Bering Strait for model years 5, 10, and 15. Flood waters from the Columbia River migrate into the Arctic through the open Bering Strait and follow boundary currents to the subpolar North Atlantic. This leads to a flushing of Arctic sea-ice and a cooling of the Gulf Stream region in response to surface freshening.

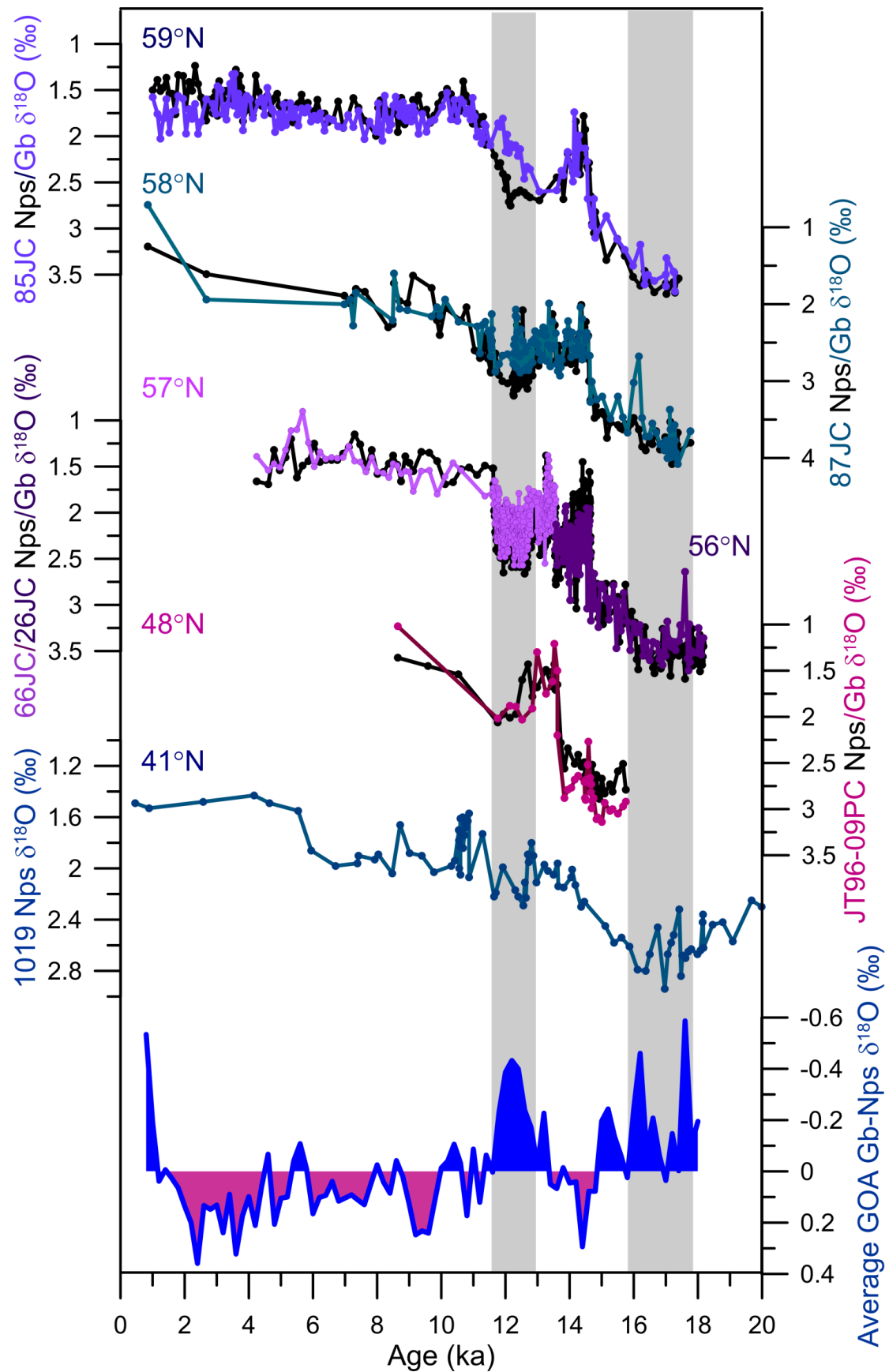


Fig. S2. Planktic $\delta^{18}\text{O}$ records from the Northeast Pacific. Data from top to bottom: EW0408-85JC (44), EW0408-87JC, EW0408-66JC (17), EW0408-26JC (17), JT96-09PC, ODP 1019 (42). Planktic species *N. pachyderma sinistral* (Nps) and *G. bulloides* (Gb). The difference between near-surface dwelling Gb and the deeper thermocline-dwelling Nps may indicate changes in near-surface stratification (with more negative values inferred to reflect greater stratification). An average Gb-Nps record was constructed by linearly interpolating the individual Gb-Nps records for each core on a 200-yr timestep and averaging the overlapping records (blue): blue shading denotes periods when Gb values are lighter than Nps, and red shading denotes periods when Nps values are heavier than Gb . The average GOA Gb-Nps record shows maximum near-surface stratification in the early deglaciation (18-16.0 ka) and YD, similar to the reconstructed $\delta^{18}\text{O}_{\text{sw-ivc}}$ (Fig. 3). Analytical error for $\delta^{18}\text{O}$ measurements are $\pm 0.04\text{\textperthousand}$.

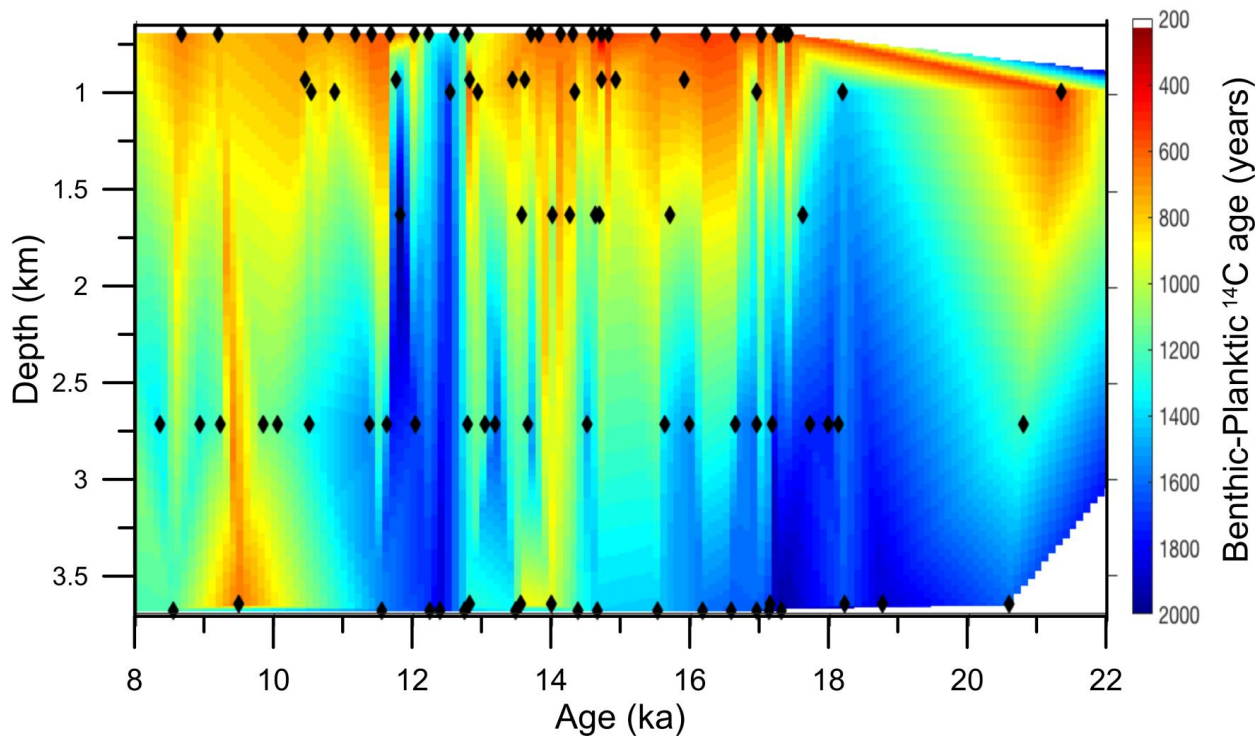


Fig. S3. Compilation of Northeastern Pacific B-P radiocarbon age differences from the LGM through the early Holocene. Same data as in Fig. 4 except the age range has been extended from 21-8 ka. Data is limited for the LGM, but the intermediate depth sites show similar B-P ages for intermediate depths (ODP 1019, W8709-13PC; 42, 43), whereas a deeper site (ODP 887) appears to have higher B-P ages during the LGM (61).

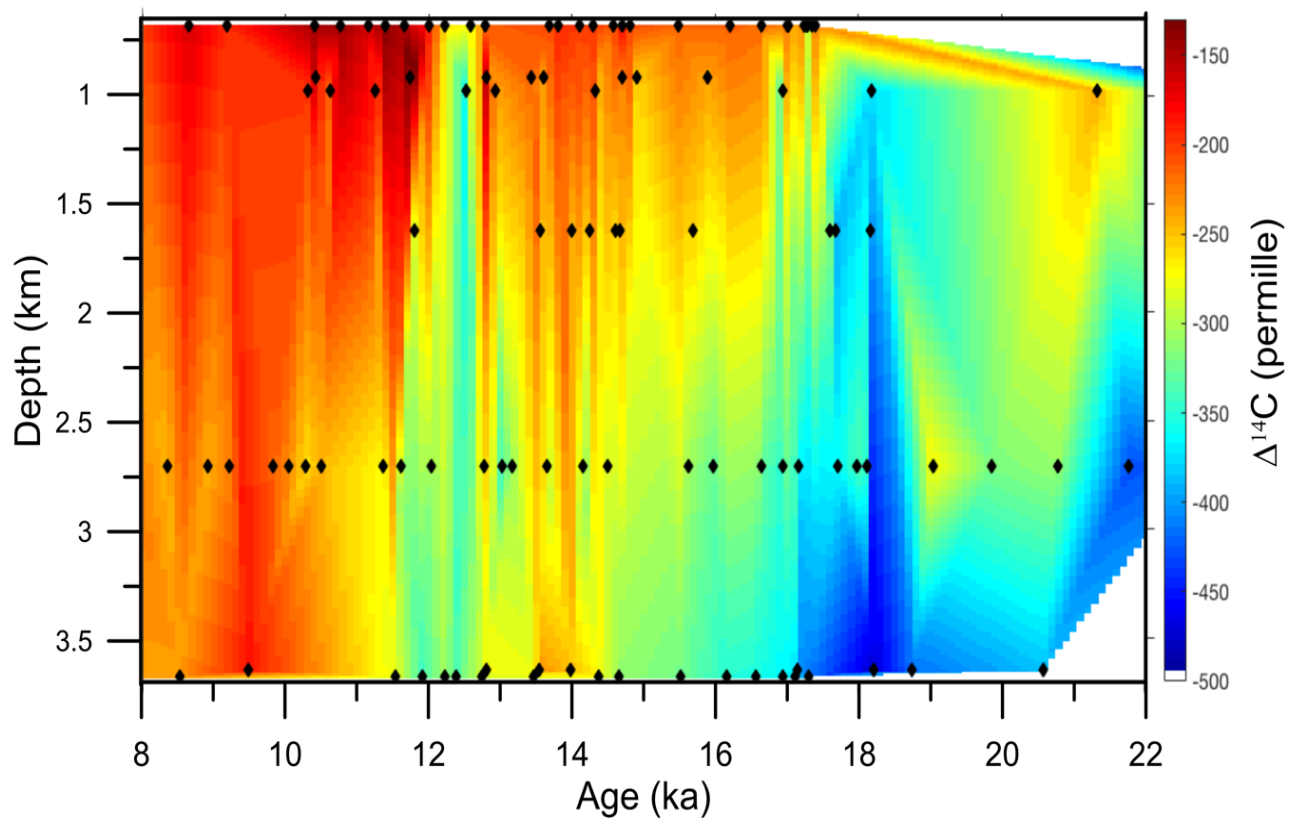


Fig. S4. Compilation of Northeastern Pacific subsurface ventilation records from the LGM through the early Holocene [with $\Delta^{14}\text{C}$ (%)] instead of B-P age differences. Subsurface radiocarbon anomalies, expressed here as $\Delta^{14}\text{C}$ relative to contemporaneous atmospheric $\Delta^{14}\text{C}$, occur at the same time as greater B-P age differences (Fig. 4, fig. S3), which occur from 19-17 ka and 13-12ka.

Table S1. A revised mean composite depth for the upper 8 m of ODP core 1019A based on a revised correlation of GRA and MS data to the other cores within the splice for the upper 7 m. The RMCD for the section between 7-8 mcd was based on correlation of the UK'37 SST record in core 1019A to the UK'37 SST record in 1019C, in which no changes were made to the original shipboard MCD.

Core	1019A MCD	1019A RMCD	1019A Affine	Notes	Revised correlation
1H	2.48	2.73	0.25	disturbed	GRA & MS data
1H	2.92	3.16	0.24	disturbed	GRA & MS data
1H	3.20	3.43	0.23	disturbed	GRA & MS data
1H	3.72	4.03	0.31	disturbed	GRA & MS data
1H	4.10	4.35	0.25	disturbed	GRA & MS data
1H	4.42	4.65	0.23	disturbed	GRA & MS data
1H	4.50	4.75	0.25	disturbed	GRA & MS data
1H	4.69	4.90	0.21		GRA & MS data
1H	4.78	5.09	0.31		GRA & MS data
1H	4.87	5.21	0.34		GRA & MS data
1H	4.91	5.23	0.32		GRA & MS data
1H	4.97	5.28	0.31		GRA & MS data
1H	5.02	5.36	0.34		GRA & MS data
1H	5.07	5.40	0.33		GRA & MS data
1H	5.17	5.47	0.30		GRA & MS data
1H	5.22	5.48	0.26		GRA & MS data
1H	5.27	5.48	0.21		GRA & MS data
1H	5.32	5.49	0.17		GRA & MS data
1H	5.37	5.53	0.16		GRA & MS data
1H	6.07	6.09	0.02		GRA & MS data
1H	6.12	6.18	0.06		GRA & MS data
1H	6.17	6.27	0.10		GRA & MS data
1H	6.22	6.34	0.12		GRA & MS data
1H	6.27	6.43	0.16		GRA & MS data
1H	6.32	6.49	0.17		GRA & MS data
1H	6.37	6.53	0.16		GRA & MS data
1H	6.42	6.56	0.14		GRA & MS data
1H	6.62	6.75	0.13		GRA & MS data
1H	6.93	7.01	0.08		GRA & MS data
1H	6.98	7.04	0.06		SST correlation to 1019C
1H	7.93	7.98	0.05		SST correlation to 1019C
1H	8.03	8.03	0.00		original MCD

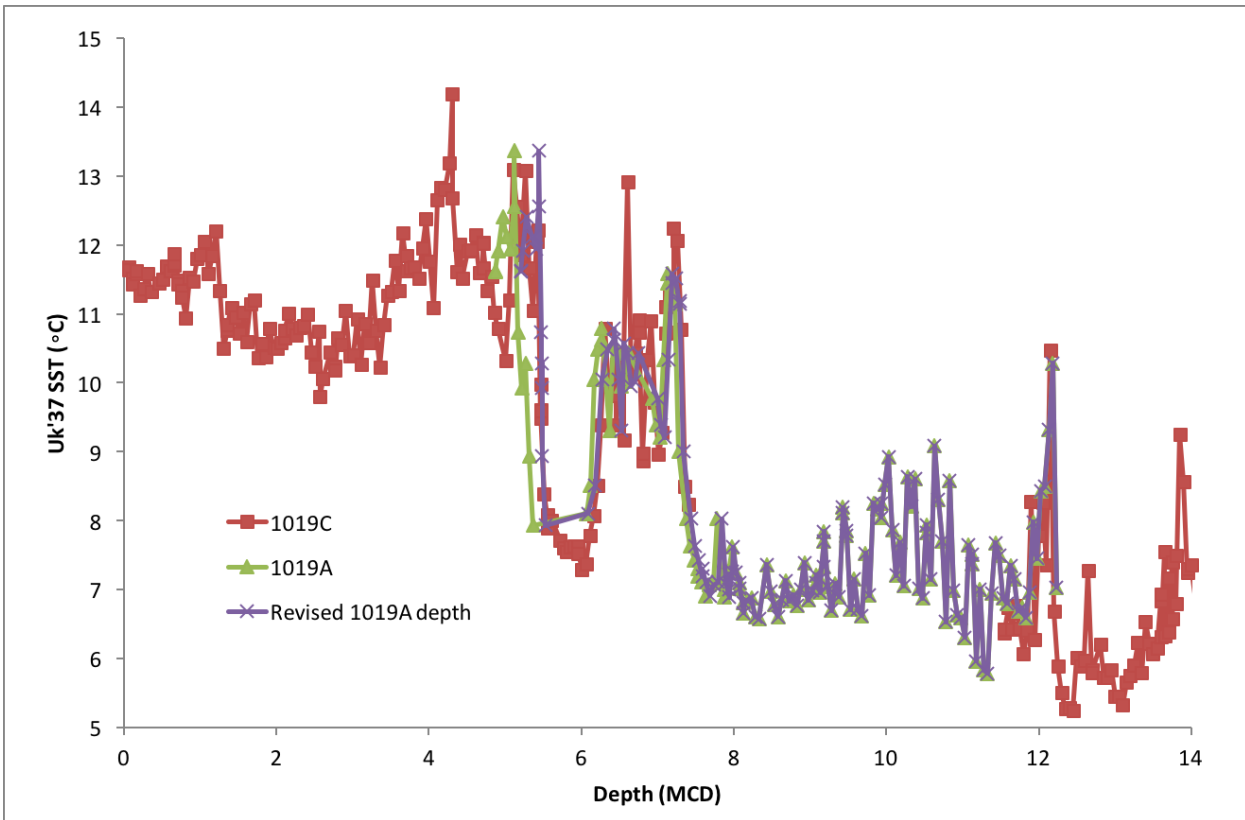


Fig. S5. SST measurements for ODP cores 1019C and 1019A on the original mean core depth splice (red, 1019C; green, 1019A) show misalignment near the Holocene transition by ~30 cm and the BA and YD transitions by ~5 cm. A revised MCD for hole 1019A was produced by correlation between the magnetic susceptibility and GRA records of the upper section of core 1019A (2.5-7.0 MCD) to core 1019C, and a correlation of the SST record of 1019A to 1019C between 7.0-8.0 MCD (purple) for the composite SST record.

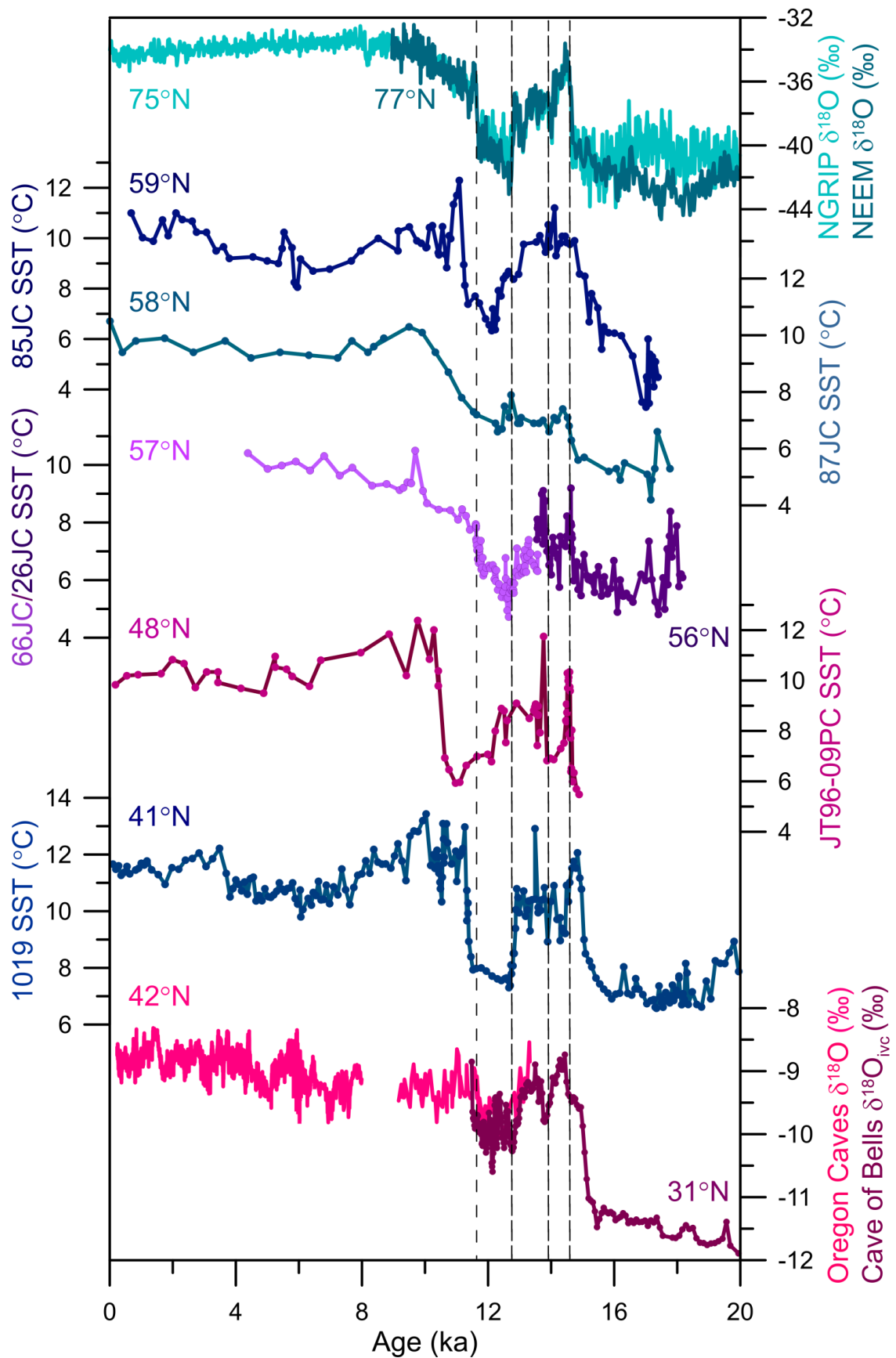


Fig. S6. Compilation of Northeast Pacific $\text{Uk}'37$ SST reconstructions on age models with constant marine reservoir correction, in comparison with annual layer counted chronologies of the Greenland ice cores (46, 53) and the absolute U-Th chronologies of the western U.S speleothem records (69–71). Dashed lines show timing of the Bølling transition, 14.0 ka climate event, YD, and Holocene transitions in the Greenland records for reference with abrupt climate transitions in the other proxies.

Table S2. Proxy data used for the global SST anomaly maps in Fig. 5 [(38, 45, 83–165) listed in alphabetic order]. For expanded metadata and site-based SST estimates, see accompanying excel metadata file.

Table S2. Proxy data used in Fig. 5				
Core	Lat (°)	Lon (°)	Proxy	Reference
MD95-2011	67.0	7.6	foram assemblages	Risebrobakken et al., 2011
MD95-2010	66.7	4.6	foram assemblages	Eldevik et al., 2014, Dokken et al., 2015
MD99-2284	62.4	-1.0	foram assemblages	Risebrobakken et al., 2011, Dokken et al., 2015
DA04-31P	62.6	-54.2	$U^{K_{37}}$	Knutz et al., 2011
RAPID-15-4P	62.3	-17.1	Mg/Ca	Thornally et al., 2010
RAPID-15-4P	62.3	-17.1	Mg/Ca	Thornally et al., 2010
SO201-2-114KL	59.3	167.0	TEX ₈₆	Meyer et al., 2016
SO201-2-114KL	59.3	167.0	$U^{K_{37}}$	Max et al., 2012
EW0408-85JC	59.6	-144.2	$U^{K_{37}}$	Praetorius et al., 2015
EW0408-87JC	58.8	-144.5	$U^{K_{37}}$	this paper (Praetorius et al., 2019)
SO201-2-101KL	58.8	170.7	Mg/Ca	Riethdorf et al., 2013
EW0408-66JC	58.5	-137.2	$U^{K_{37}}$	Praetorius et al., 2016
EW0408-26JC	57.6	-136.7	$U^{K_{37}}$	Praetorius et al., 2016
SO201-2-85KL	57.5	170.4	Mg/Ca	Riethdorf et al., 2013
SO201-2-85KL	57.5	170.4	$U^{K_{37}}$	Max et al., 2012
SO201-2-77KL	56.3	170.7	$U^{K_{37}}$	Max et al., 2012
SO201-2-77KL	56.3	170.7	Mg/Ca	Riethdorf et al., 2013
NA87-22	55.5	-14.7	foram assemblages	Waelbroeck et al., 2001
ODP 980	55.5	-14.7	Mg/Ca	Benway et al., 2010
ODP 980	55.5	-14.7	foram assemblages	Benway et al., 2010
Healy-02-02-51JPC	54.6	-168.7	$U^{K_{37}}$	Caissie et al., 2010
SO201-2-12KL	54.0	162.4	TEX ₈₆	Meyer et al., 2016
SO201-2-12KL	54.0	162.4	Mg/Ca	Riethdorf et al., 2013
SO201-2-12KL	54.0	162.4	$U^{K_{37}}$	Max et al., 2012
MD01-2461	51.8	-12.9	Mg/Ca	Peck et al., 2008
LV29-114-3	49.4	152.9	$U^{K_{37}}$	Max et al., 2012
LV29-114-3	49.4	152.9	Mg/Ca	Riethdorf et al., 2013
PC-04	49.4	153.0	$U^{K_{37}}$	Harada et al., 2004
MD02-2496	49.0	-127.0	Mg/Ca	Taylor et al., 2014
MD02-2496	49.0	-127.0	Mg/Ca	Taylor et al., 2014
JT96-96	48.9	-126.9	$U^{K_{37}}$	Kienast & McKay 2001
MD95-2002	47.5	-8.5	foram assemblages	Eynaud et al., 2012
MD95-2002	47.5	-8.5	dinocyst assemblages	Eynaud et al., 2012
PC-01	46.3	152.5	$U^{K_{37}}$	Harada et al., 2004
MD01-2412	44.5	145.0	$U^{K_{37}}$	Harada et al., 2006
P178-15P	44.3	12.0	$U^{K_{37}}$	Tierney et al., 2016
P178-15P	44.3	12.0	Mg/Ca	Tierney et al., 2016
P178-15P	44.3	12.0	TEX ₈₆	Tierney et al., 2016
OMEXII-9K	42.3	-10.1	foram assemblages	Salgueiro et al., 2014
MD03-2697	42.2	-9.7	foram assemblages	Salgueiro et al., 2014
MD99-2331	42.2	-9.7	foram assemblages	Salgueiro et al., 2014
CH 69-09	41.8	-47.4	foram assemblages	Waelbroeck et al., 2001
ODP1019	41.7	-124.9	$U^{K_{37}}$	Barron et al., 2003, Herbert et al., 2003

Table S2. Continued...				
306-U1313B	41.0	-33.0	$U^{K'_{37}}$	Naafs et al., 2012
MD95-2040	40.8	-9.9	foram assemblages	Salgueiro et al., 2014
MD95-2039	40.6	-10.4	foram assemblages	Salgueiro et al., 2014
PC-6	40.4	143.5	$U^{K'_{37}}$	Minoshima et al., 2007
MD01-2446	39.1	-12.6	foram assemblages	Salgueiro et al., 2014
MD03-2699	39.0	-10.7	$U^{K'_{37}}$	Rodrigues et al., 2010
D13882	38.6	-9.5	$U^{K'_{37}}$	Rodrigues et al., 2010
BS79-38	38.4	13.6	$U^{K'_{37}}$	Cacho et al., 2001
MD95-2042	37.8	-10.2	foram assemblages	Salgueiro et al., 2014
SU81-18	37.8	-10.2	$U^{K'_{37}}$	Bard et al., 2000
SU81-18	37.8	-10.2	foram assemblages	Waelbroeck et al., 2001
MD95-2037	37.1	-32.0	$U^{K'_{37}}$	Calvo et al., 2001
M39-008	36.4	-7.1	$U^{K'_{37}}$	Cacho et al., 2001
MD95-2043	36.1	-2.6	$U^{K'_{37}}$	Cacho et al., 1999
M39029-7	36.0	-8.2	foram assemblages	Salgueiro et al., 2014
MD01-2421	36.0	141.8	$U^{K'_{37}}$	Isono et al., 2009
MD99-2339	35.9	-7.5	foram assemblages	Salgueiro et al., 2014
ODP 1017	34.5	-121.1	Mg/Ca	Pak et al., 2012
ODP 1017	34.5	-121.1	foram assemblages	Hendy 2010
ODP 1017	34.5	-121.1	$U^{K'_{37}}$	Seki et al., 2002
ODP 893	34.3	-120.0	foram assemblages	Hendy 2010
OCE326-GGC5	33.7	-57.6	Mg/Ca	Carlson et al., 2008
KT92-17 St. 14	32.6	138.6	$U^{K'_{37}}$	Sawada and Handa, 1998
KNR140-51GGC	32.6	-76.3	Mg/Ca	Carlson et al., 2008
KY07-04-01	31.6	128.9	Mg/Ca	Kubota et al., 2010
MD98-2195	31.6	129.0	$U^{K'_{37}}$	Ijiri et al., 2005
MD02-2575	29.0	-87.1	Mg/Ca	Ziegler et al., 2008
GeoB 5844-2	27.7	34.7	UK'37	Arz et al., 2003
MD02-2515	27.5	-112.1	UK'37	McClymont et al., 2012
MD02-2515	27.5	-112.1	TEX ₈₆	McClymont et al., 2012
EN32-PC6	27.0	-91.3	Mg/Ca	Flower et al., 2004
MD02-2550	27.0	-91.4	Mg/Ca	Williams et al., 2010
MD02-2550	27.0	-91.4	Mg/Ca	Williams et al., 2010
KNR166-2-26JPC	24.3	-83.3	Mg/Ca	Schmidt & Lynch-Steiglitz 2011
ODP 658C	20.8	-18.6	foram assemblages	deMenocal et al., 2000
ODP 658C	20.8	-18.6	$U^{K'_{37}}$	Zhao et al., 1995
17940	20.1	117.4	$U^{K'_{37}}$	Pelejero et al., 1999
ODP 1144	20.1	117.6	Mg/Ca	Wei et al, 2007
GeoB 9508-5	15.5	-18.0	$U^{K'_{37}}$	Niedermeyer et al., 2009
GeoB 9508-5	15.5	-18.0	Mg/Ca	Zarriess et al., 2011
74KL	14.3	57.3	$U^{K'_{37}}$	Huguet et al., 2006
74KL	14.3	57.3	TEX ₈₆	Huguet et al., 2006
GeoB9526	12.4	-18.1	Mg/Ca	Zarriess et al., 2011
M35003-4	12.1	-61.3	$U^{K'_{37}}$	Rühlemann et al., 1999

Table S2. Continued...				
VM28-122	11.6	-78.4	Mg/Ca	Schmidt et al., 2004
SK237-GC04	11.0	75.0	Mg/Ca	Saraswat et al., 2013
NIOP-905	10.8	51.9	$U^{K_{37}}$	Huguet et al., 2006
NIOP-905	10.8	51.9	TEX ₈₆	Huguet et al., 2006
PL07-39PC	10.7	-65.0	Mg/Ca	Lea et al., 2003
MD97-2141	8.8	121.3	Mg/Ca	Rosenthal et al., 2003
MD02-2529	8.2	-84.1	$U^{K_{37}}$	Leduc et al., 2007
ME0005A-43JC	7.9	-83.6	Mg/Ca	Benway et al., 2006
MD01-2390	6.6	113.4	$U^{K_{37}}$	Steinke et al., 2008
MD01-2390	6.6	113.4	Mg/Ca	Steinke et al., 2008
MD98-2181	6.3	125.8	Mg/Ca	Stott et al., 2007
MD03-2707	2.5	9.4	Mg/Ca	Weldeab et al., 2007
GeoB 4905	2.5	9.4	Mg/Ca	Weldeab et al., 2005
TR163-22	0.5	-92.4	Mg/Ca	Lea et al., 2006
ME0005A-24JC	0.0	-86.5	$U^{K_{37}}$	Kienast et al., 2006
V21-30	-1.2	-89.7	$U^{K_{37}}$	Koutavas and Sachs, 2008
V21-30	-1.2	-89.7	Mg/Ca	Koutavas et al., 2002
GeoB 3910	-4.2	-36.3	$U^{K_{37}}$	Jaeschke et al., 2007
GeoB 3129	-4.6	-36.6	Mg/Ca	Weldeab et al., 2006
MD98-2162	-4.7	117.9	Mg/Ca	Visser et al., 2003
MD98-2176	-5.0	133.4	Mg/Ca	Stott et al., 2007
GeoB 6518-1	-5.6	11.2	MBT/CBT	Weijers et al., 2007
GeoB 6518-1	-5.6	11.2	$U^{K_{37}}$	Schefuß et al., 2005
GeoB10069-3	-9.6	120.9	Mg/Ca	Gibbons et al., 2014
MD98-2165	-9.7	118.4	Mg/Ca	Levi et al., 2007
MD98-2170	-10.6	125.4	Mg/Ca	Stott et al., 2007
MD01-2378	-13.1	121.8	Mg/Ca	Xu et al., 2008
GeoB 1023-5	-17.2	11.0	$U^{K_{37}}$	Kim et al., 2002
MD79-257	-20.4	36.3	$U^{K_{37}}$	Bard et al., 1997
ODP 1084B	-25.5	13.0	Mg/Ca	Farmer et al., 2005
KNR159-5-36GGC	-27.5	-46.5	Mg/Ca	Carlson et al., 2008
GeoB 7139-2	-30.2	-72.0	$U^{K_{37}}$	Kaiser et al., 2008
GeoB 3359-3	-35.2	-72.8	$U^{K_{37}}$	Romero et al., 2006
GeoB 7165-1	-36.6	-73.7	$U^{K_{37}}$	Mohtadi et al., 2008
MD03-2611	-36.7	136.7	$U^{K_{37}}$	Calvo et al., 2007
MD03-2607	-37.0	137.4	$U^{K_{37}}$	Lopes dos Santos et al., 2013
MD03-2607	-37.0	137.4	TEX ₈₆	Lopes dos Santos et al., 2013
MD03-2607	-37.0	137.4	foram assemblages	Lopes dos Santos et al., 2013
MD97-2121	-40.4	178.0	$U^{K_{37}}$	Pahnke and Sachs, 2006
ODP 1233	-41.0	-74.5	$U^{K_{37}}$	Lamy et al., 2007
TN057-21-PC2	-41.1	7.8	$U^{K_{37}}$	Sachs et al., 2001
TN057-21	-41.1	7.8	Mg/Ca	Barker et al., 2009
TN057-06-PC4	-42.9	8.9	$U^{K_{37}}$	Anderson et al., 2014
SO136-GC11	-43.5	167.9	$U^{K_{37}}$	Barrows et al., 2007

Table S2. Continued...				
MD97-2120	-45.5	174.9	$U^{K'}_{37}$	Pahnke and Sachs, 2006
MD94-103	-45.6	86.5	$U^{K'}_{37}$	Sicre et al., 2005
MD88-770	-46.0	96.5	foram assemblages	Labeyrie et al., 1996
MD07-3088	-46.1	-74.7	foram assemblages	Sani et al., 2013